

# PREDICTION OF SHRINKAGE AND CREEP STRESSES IN CONCRETE REPAIR SYSTEMS

A.H. Al-Gadhib, M.K. Rahman and M.H. Baluch

Department of Civil Engineering  
King Fahd University of Petroleum & Minerals  
Dhahran 31261, Saudi Arabia

## ABSTRACT

This paper addresses the problem of stress buildup in the repair layer of a concrete patch repair system resulting from moisture diffusion. As moisture evaporates from the repair layer into the surrounding ambience of known relative humidity, the hardened concrete substrate restrains free shrinkage movement of the repair layer. As a consequence, primary tensile stresses are set up in the repair layer together with shear and peeling stresses at the repair/concrete substrate interface.

As a secondary effect, the restraint exercised by the substrate on the resulting tensile creep deformation of the repair layer results in a stress field of reversed sense as that occurring due to restrained shrinkage. The secondary stresses due to restrained creep serve to relieve the primary shrinkage associated stress field, and the net or total stress buildup as a result is reduced.

Finite element models are used both for moisture diffusion and for computing the resulting stresses due to restrained shrinkage and tensile creep. An empirical expression for creep strain  $\epsilon_{cr}$ , based on the elastic strain resulting from the tensile stress due to restrained shrinkage, is inputted to yield the resulting stress field due to restrained creep. Superposition of stresses due to restrained shrinkage and creep yield the net stress buildup at any time. Possible zones of failure are identified in the repair layer and at the interface of the patch repair system.

## KEYWORDS

Computational model, moisture diffusion, restrained shrinkage, tensile creep, patch concrete repair.

## 1.0 INTRODUCTION

As articulated by Cusson and Mailvaganam (1996), the lack of durability (or more accurately the lack of compatibility) in repaired structures manifests itself in spalling, cracking, scaling and subsequent loss of strength. Three major modes of failure in concrete patch repair systems have been identified to include:

- \* tensile cracking through the thickness of the patch repair layer
- \* shearing of the substrate concrete below the interface of the repair and the substrate concrete
- \* failure of interface between repair layer and substrate concrete

The process of diffusion of moisture from the repair layer of the patch system activates a chain of events leading to build up of normal and shear stresses in the repair/substrate composite. This sequence at any time interval  $t = t_1$  includes:

- \* shrinkage strains in repair layer as a consequence of moisture loss
- \* build up of stresses in both repair layer and concrete substrate as the repair layer is constrained by the substrate, and the drying shrinkage strains are not allowed to occur freely. The repair layer normal stress build up is tensile, whereas the substrate is subjected to compressive stresses
- \* the repair layer, under the sustained action of the tensile stress field, wants to creep by virtue of the presence of moisture in it. However, this creep deformation is not allowed to occur freely - yet again a consequence of the substrate concrete imposing a constraint
- \* the restraint offered to creep deformation in the patch system results now in stresses of sense opposite to those under restrained shrinkage i.e. compressive in the repair layer and tensile in the substrate. This in literature is referred to as stress relief due to creep.

The net stress field at time  $t = t_1$  is the combined effect of stresses due to restrained shrinkage and restrained creep.

In view of the mechanism that governs the build up of stresses due to restrained shrinkage and creep, it is apparent that several characteristic properties of the repair layer and the substrate combine to influence the magnitude of the stress field at various time increments. Emberson and Mays (1990), in discussing requirements for installation of a repair layer compatible with the concrete substrate, recommend the relative magnitudes of various material properties as shown in Table 1.

Cement-based materials shrink as a consequence of loss of moisture whereas resin based materials shrink as a result of cooling following the initial exothermic reaction (Brill, Komlos and Najzalan (1980)). In a patch repair system, the concrete substrate is usually mature and the hardened concrete offers restraint to the repair layer in not allowing it to shrink freely.

Property	Relationship of Repair Layer (R) to Substrate (S)
Shrinkage Strain	$\epsilon_{sh}^R < \epsilon_{sh}^S$
Creep Coefficient (Repair in Tension)	$\epsilon_{cr}^t R > \epsilon_{cr}^t S$
Creep Coefficient (Repair in Compression)	$\epsilon_{cr}^c R < \epsilon_{cr}^c S$
Thermal Expansion Coefficient	$\alpha_R = \alpha_S$
Modulus of Elasticity	$E_R = E_S$
Poisson's Ratio	$\nu_R = \nu_S$
Tensile Strength	$f_t^R > f_t^S$

Table 1: Recommended Patch Properties

In total absence of restraint, the repair layer would shrink freely with no development of stress. Stress develops due to restraint, and its magnitude depends on the potential of the material to shrink freely as indicated by the ultimate free shrinkage strain  $\epsilon_{sh}^R$ . The smaller the value of  $\epsilon_{sh}^R$ , the lower will be the tensile stress developed in the patch layer in order to make the deformation of the patch compatible with that of the substrate.

If the final loading on a repair system is expected to result in tensile stresses in the repair layer, the stress relief by virtue of creep of the repair layer must come by superposing a compressive stress field. The relative free creep strain ( $\epsilon_{cr}^t R - \epsilon_{cr}^t S$ ) should be  $> 0$ , in order to ensure development of compression in repair layer and tension in substrate for compatible deformation. Conversely, if the repair layer is expected to be functioning in compression eventually, the stress relief due to creep will occur only if ( $\epsilon_{cr}^t R - \epsilon_{cr}^c S$ )  $< 0$ .

If one was to assume the adoption of a repair material with matching elastic modulus, Poisson's ratio and coefficient of thermal expansion, the properties of repair materials including cementitious mortars, polymer-modified cementitious mortars and resinous mortars that would dictate the performance of the patch system would be (i) drying shrinkage strain  $\epsilon_{sh}$ , (ii) tensile creep strain  $\epsilon_{cr}$ , (iii) tensile modulus of elasticity ( $E_t$ ) and (iv) tensile strength ( $f_t$ ).

It is only recently that it has been recognized that predicting performance of a repair patch system based on the index of compressive strength is an exercise in futility [Pinelle (1995)]. According to Pinelle, predicting the cracking tendency of repair mortars using the parameter of compressive strength was as reliable as using Newton's laws of motion developed for rigid bodies for predicting behavior of light (as Newton had attempted!).

Although the problem of moisture diffusion and the associated phenomenon of drying shrinkage has been studied extensively in concrete alone [Sakata (1993), Penev & Kawamura (1991) and Iding & Bresler (1982)], it is only recently that a series of papers by Emmons and his co-workers [Emmons, Vaysburd and McDonald (1993, 1994), Emmons and Vaysburd (1994 a,b) and Emmons et al (1995)] has given impetus and new direction to researchers in the area of concrete repair. Literature addressing tensile creep and its measurement in concrete type materials is now making its presence [Kovler (1994), Bissonnette and Pigeon (1995)] revealing the new thinking amongst the experts in concrete repair. A computational model to quantify stress build up due to substrate restraint in a repair system utilizing finite element methodology for prediction of both moisture diffusion and associated stress build up due to restrained shrinkage has been recently proposed by Asad, Baluch and Al-Gadhib (1997).

## 2.0 PREDICTION OF MOISTURE DISTRIBUTION IN CEMENTITIOUS REPAIR MATERIALS

### 2.1 Mathematical Model for Moisture Diffusion

The mathematical model for moisture diffusion is based on the assumption that moisture flow within a cementitious material obeys the moisture diffusion equation. The diffusion equation which is the governing differential equation for moisture flow in porous materials is given by Fick's second law as

$$\frac{\partial C}{\partial t} = \frac{\partial}{\partial x} \left\{ K_c(C) \frac{\partial C}{\partial x} \right\} + \frac{\partial}{\partial y} \left\{ K_c(C) \frac{\partial C}{\partial y} \right\} + \frac{\partial}{\partial z} \left\{ K_c(C) \frac{\partial C}{\partial z} \right\} \quad (1)$$

where  $C(x,y,z,t)$  is the moisture content,  $K_c$  is the moisture diffusivity and  $t$  is the time from start of diffusion process.

The moisture diffusivity  $K_c$  is a material property and can be defined as the rate at which the moisture flows through the material when there exists a unit moisture gradient. The diffusivity  $K_c$  is highly moisture dependent which renders the moisture diffusion problem through any porous medium nonlinear.

To solve equation (1), one needs the following initial and boundary conditions:

$$C(x,y,z,t=0) = C_o(x,y,z) \quad (2)$$

$$C = C_b, \quad \text{prescribed moisture content at boundary} \quad (3)$$

$$\frac{\partial C}{\partial n} = 0, \quad \text{on sealed boundary} \quad (4)$$

$$K_c(C) \frac{\partial C}{\partial n} = f (C_e - C_s), \text{ on surface evaporation boundary.} \quad (5)$$

where  $\frac{\partial C}{\partial n}$  is moisture gradient at the drying surface identified by a unit normal  $n$ ,

$C_e$  is the equilibrium moisture content that an element would reach given particular environmental condition,  $C_s$  is the moisture content of the drying surface, and  $f$  is value of the surface factor.

## 2.2 Finite Element Formulation

The two-dimensional moisture diffusion equation, inclusive of domain evaporation is:

$$\frac{\partial C}{\partial t} = \frac{\partial}{\partial x} \left\{ K_c(C) \frac{\partial C}{\partial x} \right\} + \frac{\partial}{\partial y} \left\{ K_c(C) \frac{\partial C}{\partial y} \right\} - GC + Q \quad (6)$$

where  $G = 2f/t$ ,  $Q = 2fC_e/t$  and  $t$  is the thickness of the body. The finite element formulation of above equation is given by:

$$[K] \{C\} + [L] \{\dot{C}\} = \{F\} \quad (7)$$

which upon integration in time domain using finite difference method, one obtains:

$$([L] + \Delta t[K])\{C\}^{t+\Delta t} = [L]\{C\}^t + \Delta t\{F\} \quad (8)$$

where  $[K]$  represents the moisture diffusivity,  $[L]$  the moisture velocity matrix,  $\{F\}$  the external moisture flow vector,  $\{C\}$  the nodal moisture content and  $\{\dot{C}\}$  the rate of change of nodal moisture control. Since the diffusivity  $K_c$  is a function of moisture content  $\{C\}$ , it changes during the solution process and therefore  $[K]$  is re-evaluated for each time step. Also, for each time step, the solution has to be obtained iteratively because the problem is nonlinear and equation (8) will not be satisfied and a residual vector  $\{\psi\}$  will exist:

$$\{\psi\} = ([L] + \Delta t[K])\{C\}^{t+\Delta t} - [L]\{C\}^t - \Delta t\{F\} \neq 0 \quad (9)$$

and the iteration process is combined until convergence is attained and that is when a norm of  $\{\psi\}$  becomes less than a specified level of tolerance. In the above model, the diffusivity parameter  $K_c$  which depends on moisture content plays an influential role in the prediction of moisture content distribution. Based on the experimental results of moisture content and the calculated diffusivity [Asad et al (1997)], it has been found that such a relation is given by

$$K_c(C) = K_o + a[C/(1-C)]^b \quad (10)$$

where  $K_o$  is diffusivity in oven dry condition and equal to  $0.1175 \text{ cm}^2/\text{day}$  and both  $a$  and  $b$  are regression parameters, taken as 0.05 and 1.878, respectively.

### 2.3 Relationship Between Moisture Loss and Free Shrinkage Strain

To obtain a relationship between free shrinkage strains and moisture loss, the free shrinkage strains are plotted against the experimentally determined moisture loss values at different depths from the drying surface and the relationship between moisture loss and free shrinkage strain is found to be not linear [Asad et al (1997)]. Thus it is not possible to predict directly the free shrinkage strains by moisture loss for this repair material, as has been the trend for shrinkage modelling in ordinary concrete. The actual relationship between free shrinkage strain and moisture loss is given by the following expression based on a regression model

$$\epsilon_{sh}(t) = \frac{M^{1.5}}{195 + M^{1.5}} (\epsilon_{sh})^\infty \quad (11)$$

In the above equation,  $\epsilon_{sh}(t)$  represents the free shrinkage strain at time  $t$ ,  $M$  the percentage loss of moisture and  $(\epsilon_{sh})^\infty$  the ultimate free shrinkage strain of the repair material.

## 3. NUMERICAL SIMULATION

As a test example, the problem of shrinkage and creep stress build up in a thin repair layer cast on top of an appreciably thick and hardened concrete substrate is considered (Fig. 1).

The first stage addresses the problem of moisture diffusion in the top repair layer. Using a two-dimensional finite element code MSTDIFF2 (Asad, Baluch and Al-Gadhib (1997)), the moisture loss percentage  $M$  was determined as a function of time  $t$ . The surface moisture transfer coefficient  $f$  used is  $0.3 \text{ cm/day}$  with the equilibrium moisture content  $C_e$  taken as 50%. It was also assumed that moisture cannot diffuse into the substrate by treating the interface as being sealed. Diffusion into surrounding ambience was allowed only from the top surface of the repair layer.

One-half of the cross-section was analyzed using a two-dimensioned finite element grid with 451 nodal points and 100-nine noded elements as shown in Fig. 1. As a consequence of the diffusion boundary conditions, spatial moisture variation is essentially reflected only through the depth of the repair layer i.e. with the  $y$ -coordinate.

The moisture loss percentage  $M$  at each time  $t$  is converted into a free shrinkage strain  $\epsilon_{sh}(t)$  as given by equation (11). The free shrinkage strain is input into a

second generation version of software STRSRSYS (Asad, Baluch and Al-Gadhib (1997)) and now referred to as SHRCPAN, which is an acronym for SHRINKAGE & CREEP ANALYSIS. This software can perform a two-dimensional stress analysis of linear elastic bodies under either mechanical loading or due to restrained thermal, shrinkage and/or creep deformations.

The presence of the restraint at the base of the repair layer leads to a build up of stresses as moisture leaves the body. These stresses, referred as shrinkage associated stresses, are tensile through the thickness of the repair layer.

A secondary effect is triggered by the presence of the tensile stresses - that of deformations due to tensile creep in the repair layer. Due to the action of basic and drying creep under the stress field due to restrained shrinkage, creep deformations will occur and which can be approximated by (Branson (1977))

$$\frac{\epsilon_{cr}(t)}{\epsilon_{el}(t)} = C_u \frac{(t - t_1)^{0.6}}{10 + (t-t_1)^{0.6}} \quad (t \geq t_1) \quad (12)$$

where  $C_u$  is, in general, a function of (i) age of concrete at load application time  $t_1$ , (ii) relative humidity of the surrounding environment, (iii) average thickness of the member, (iv) consistency of the fresh concrete, (v) content of fine aggregates and (vi) air content of fresh concrete. Implicit in this assumption is the identical variation of tensile and compressive creep deformations and the validity of the hyperbolic law for repair materials. For standard conditions,  $C_u$  can be taken as 2.35.  $\epsilon_{el}(t)$  is the elastic strain resulting from the stress field causing creep to occur.

The restraint of the patch repair system does not allow creep deformations to occur freely - resulting in a stress field of opposite sense to that due to restrained shrinkage. Thus this stress may be referred to as "relief due to creep."

#### 4.0 RESULTS AND DISCUSSION

The patch repair system (25 mm thick and 200 mm wide) modelled as described above was analyzed for two cases:

Case I	Ultimate shrinkage strain ( $\epsilon_{sh}^{\infty}$ ) 1200 $\mu s$
Case II	Ultimate shrinkage strain ( $\epsilon_{sh}^{\infty}$ ) 800 $\mu s$

The time history of stresses due to shrinkage and creep was computed in each case for a period of 30 days at an interval of 0.25 day for up to 1 day and consequent increment of 1 day up to 30 days. Response at several critical points at the top, middle and bottom of the repair and at the center line and edges of the repair system was monitored. The critical points were identified to be Gauss point 900 at the top of the center line of repair and Gauss point 1 at the bottom of the repair [Fig. 1(c)].

Figure [2] shows the variation of  $\sigma_{xx}$  across the width for Case I at the top of the repair at time  $t = 10$  days. The shrinkage stress, the relaxation due to creep and the total stresses are shown. It can be seen from the figure that at the critical point near center line of the repair, the shrinkage stresses are decreased from 7.2 MPa to 5.8 MPa due to creep relief.

The variation across the width of repair of the stresses  $\sigma_{yy}$  at the interface, which tends to peel the repair off the substrate when tensile in nature, is shown in Figure [3]. The figure shows that there exists a zone at the edge of the repair system which is subjected to high peeling stresses of the order of 9 MPa after relaxation. These peeling stresses reduce in magnitude and change from tensile to compressive as one moves away from the edge.

Figure [4] shows the variation of shear stress at the interface across the width. It can be seen that at the edges of the repair, significant shear stresses exist which gradually decrease towards the center. From Figures [3] and [4] and the variation of  $\sigma_{xx}$  at interface (not shown), it can be seen that a biaxial tensile and shear state of stress exists at the edge of the interface.

The variation of total tensile stress  $\sigma_{xx}$  across the depth at the center of repair at various times is shown in Figure [5]. This figure shows that the tensile stresses grow across the depth as time progresses. In the top layers, the build up of tensile stresses occurs at a faster rate due to enhanced rate of moisture diffusion. This growth at the top continues up to around 20 days at which time the combined effect of decreasing (incremental) moisture loss and creep relaxation leads to decreased total tensile stress.

Figure [6] shows the temporal build up of tensile stresses  $\sigma_{yy}$  at GP 1 for material with high ultimate shrinkage strain (1200  $\mu$ s) and a material with moderately high ultimate shrinkage strain (800  $\mu$ s). It can be seen from the figure that tensile stress of the order of 12 MPa is developed in the former material which is reduced to less than 8 MPa for the latter. In both cases, however, the stresses are high enough to result in delamination at the edges and to lead to a progressive failure resulting in complete delamination at the interface. The variation of stress  $\tau_{xy}$  at the same Gauss Point (GP 1) for the two materials is shown in Figure [7]. The figure shows a continuous nonlinear growth in shear stress up to the monitored time level.

The time variation of the stress  $\sigma_{xx}$  at Gauss Point 900, Fig. [1c] for the above materials and the development of the tensile strength of the material is shown in Figure [8]. From the figure, it can be seen that for the material with higher ultimate shrinkage strain, the tensile stress at earlier ages is below the tensile capacity of the repair. At time  $t = 5$  days, the tensile stresses developed in the system exceeds the tensile capacity and will result in development and growth of tensile cracks. On the other hand, in the material with moderate ultimate shrinkage strain (800 $\mu$ s), the tensile stresses remain below the tensile capacity of the material for up to 12 days. The difference between the tensile capacity and the tensile stress in build up of the repair is, however, small. This suggests that for preventing distress in the repair

system, the free shrinkage strain is a critical material parameter.

Shown in Fig. [9] are the possible modes of failure in the patch repair, including delamination initiating at the interface edge due to combined peeling and shear stress together with tension associated cracking through the repair layer.

## 5.0 CONCLUSION

Critical zones and possible modes of failure in a patch repair system have been identified using a finite element based computational model developed to address stress build up in concrete patch repair systems due to moisture diffusion. Repair material parameters influencing rate of moisture diffusion are identifiable, forming the nascent basis for development of guidelines for rational design of repair.

## 6.0 ACKNOWLEDGEMENTS

The support of the Department of Civil Engineering and King Fahd University of Petroleum & Minerals in the pursuit of this work is acknowledge with thanks; also, the support of Fosam Company Limited in Dammam in the form of free supply of repair materials for laboratory component of research work is gratefully acknowledged.

## 7.0 REFERENCES

1. Cusson, D. and Mailvaganam, V. (1996), "Durability of Repair Materials," *Concrete International*, pp. 34-38.
2. Emberson, N.K. and Mays, G.C. (1990), "Significance of Property Mismatch in the Patch Repair of Structural Concrete - Part I: Properties of Repair Systems," *Magazine of Concrete Research*, V. 42, No. 152, pp. 147-160.
3. Brill, L., Komlos, K., and Najzalan, B. (1980), "Early Shrinkage of Cement Paste, Mortars and Concrete," *Materials & Structures*, V. 13, No. 73, pp. 41-45.
4. Pinelle, D.J. (1995), "Curing Stresses in Polymer-Modified Repair Mortars," *Cement, Concrete & Aggregates*, V. 17, No. 2, pp. 195-200.
5. Sakata, K. (1993), "A Study of Moisture Diffusion in Drying and Drying Shrinkage of Concrete," *Cement and Concrete Research*, Vol. 13, No. 2, pp. 216-224.
6. Penev, D. and Kawamura, M. (1991), "Moisture Diffusion in Soil-Cement Mixtures and Compacted Lean Concrete," *Cement and Concrete Research*, Vol. 21, No. 1, pp. 137-146.

7. Iding, R. and Bresler, B. (1982), "Prediction of Shrinkage Stresses and Deformations in Concrete," In *Fundamental Research on Creep and Shrinkage of Concrete*, ed. by Wittmann, F.H., pp. 341-352, Martinus Nijhoff Pub., The Hague, 1982.
8. Emmons, P.H. Vaysburd, A.M., and McDonald, J.E. (1993), "A Rational Approach to Durable Concrete Repairs," *Concrete International*, Vol. 15, No. 9, pp. 40-45.
9. Emmons, P.H. Vaysburd, A.M. and McDonald, J.E. (1994), "Concrete Repair in the Future Turn of the Century - Any Problems?," *Concrete International*, Vol. 16, No. 3, pp. 42-49.
10. Emmons, P.H. and Vaysburd, A.M. (1994a), "Factors Affecting the Durability of Concrete Repair: The Contractor's Viewpoint," *Construction and Building Materials*, Vol. 8, No. 1, pp. 5-16.
11. Emmons, P.H. and Vaysburd, A.M. (1994b), "The Total System Concept - Necessary for Improving the Performance of Repaired Structures," *Concrete International*, Vol. 17, No. 3, pp. 31-36.
12. Emmons, P.H. Vaysburd, A.M., Pinelle, D.J., Poston, R.W., and Walkowicz, S. (1995), "The Origin of Durability of Concrete Repairs," *International Association for Bridge and Structural Engineering Symposium*, San Francisco.
13. Kovler, K. (1994), "Testing System for Determining the Mechanical Behavior of Early Age Concrete Under Restrained & Free Uniaxial Shrinkage," *Materials & Structures*, V. 27, pp. 324-330.
14. Bissonnette, B. & Pigeon, M. (1995), "Tensile Creep at Early Ages of Ordinary Silica Fume, and Fiber Reinforced Concretes," *Cement & Concrete Research*, Universite Laval, Quebec.
15. Asad, M., Baluch, M.H. and Al-Gadhib, A.H. (1997), "Drying Shrinkage Stresses in Restrained Concrete Systems," *Magazine of Concrete Research*, to appear.
16. Branson, D.E., "Deformations of Concrete Structures," New York: McGraw-Hill, 1977.

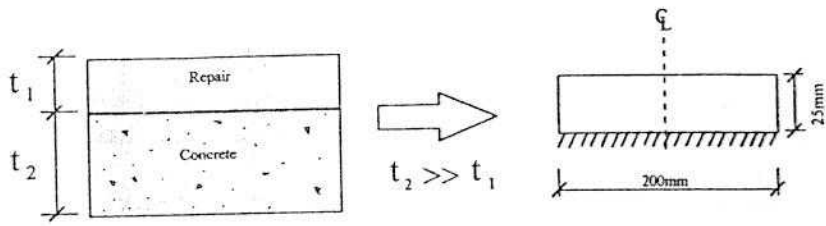


Fig. 1 (a) Patch Repair System

Fig. 1 (b) Equivalent Model

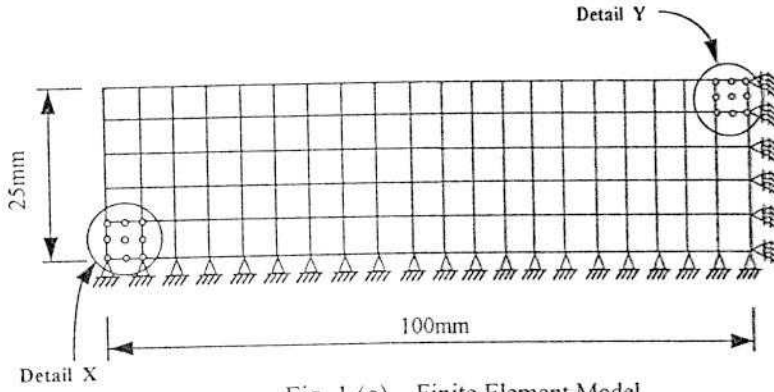
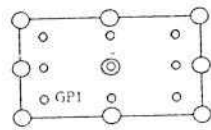
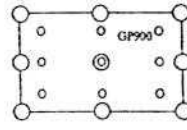


Fig. 1 (c) Finite Element Model



Detail X  
Element # 1



Detail Y  
Element # 100

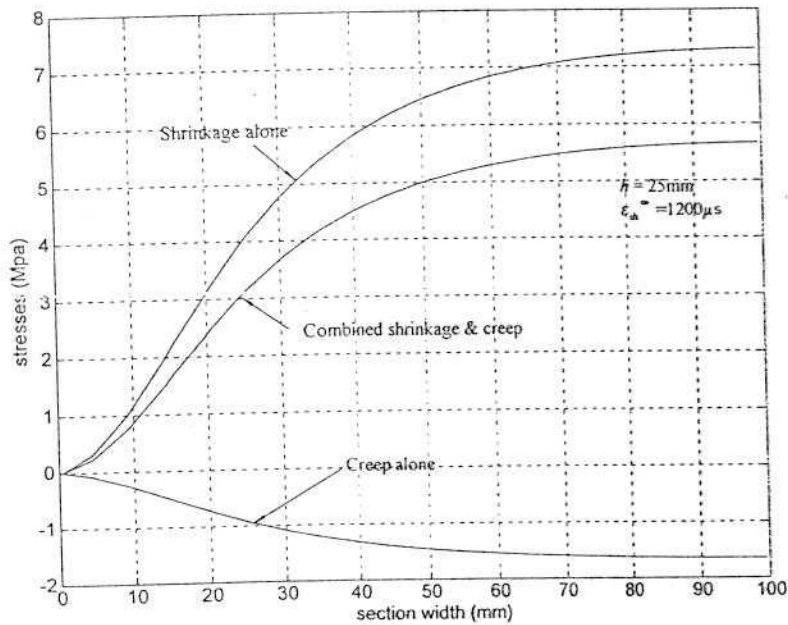


Fig. 2: Variation of  $\sigma_{xx}$  across width at top ( $t = 10$  days)

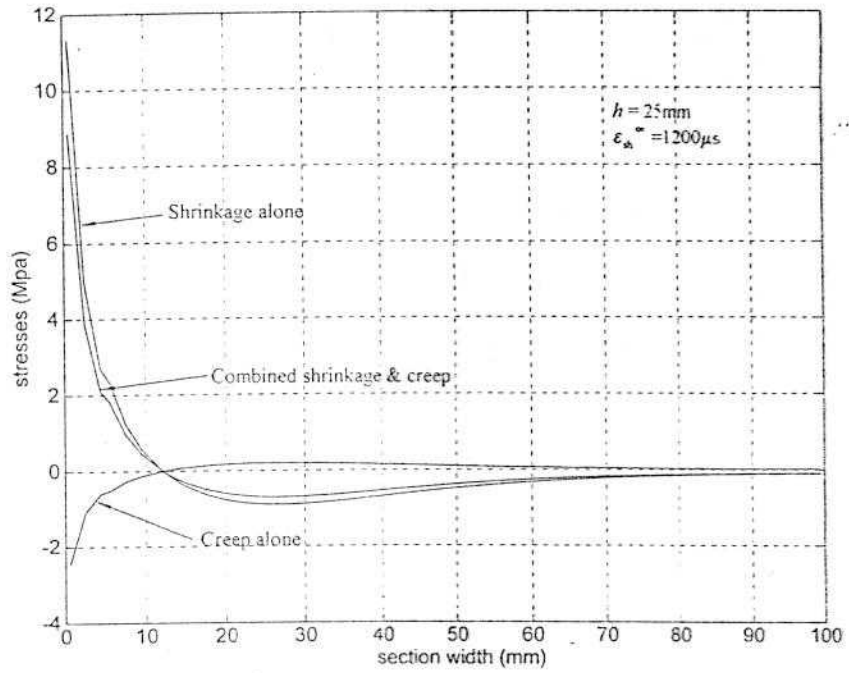


Fig. 3: Variation of  $\sigma_{xx}$  across width at Interface ( $t = 10$  days)

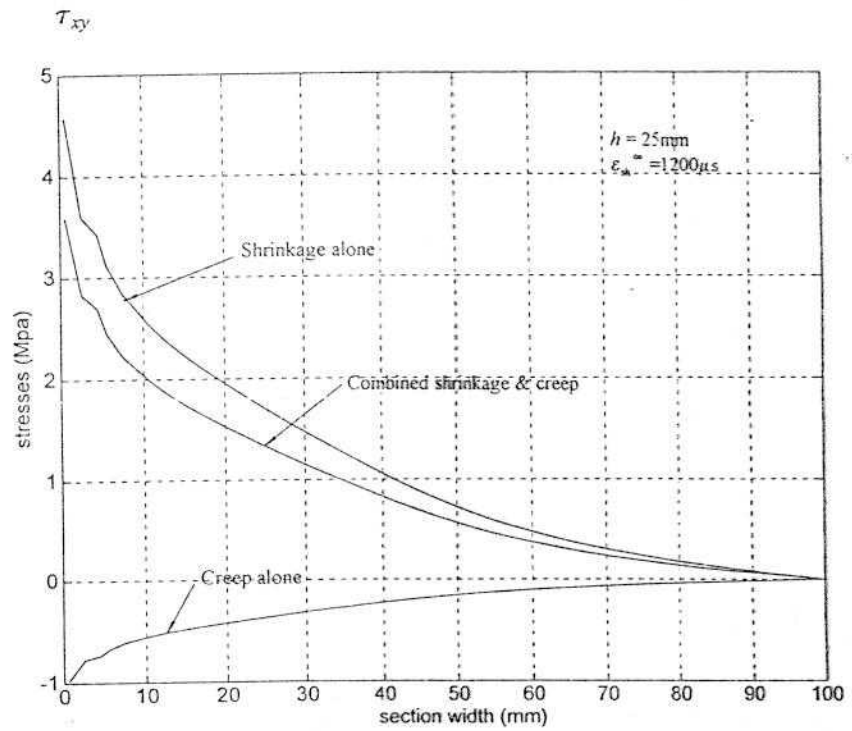


Fig. 4: Variation of shear stress  $T_{xy}$  across width at interface ( $t = 10$  days)

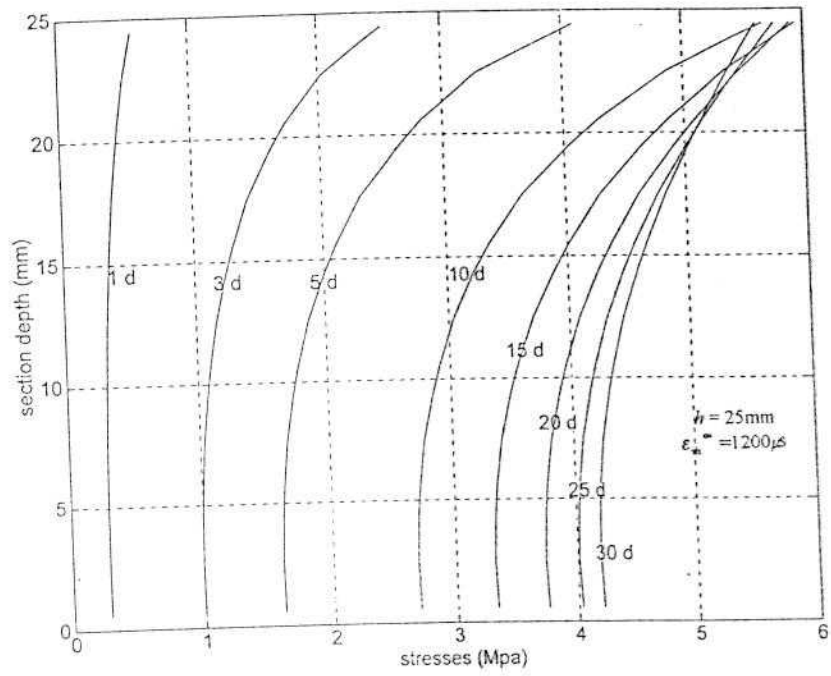


Fig. 5: Variation of  $\sigma_{xx}$  across depth at repair center at various times.

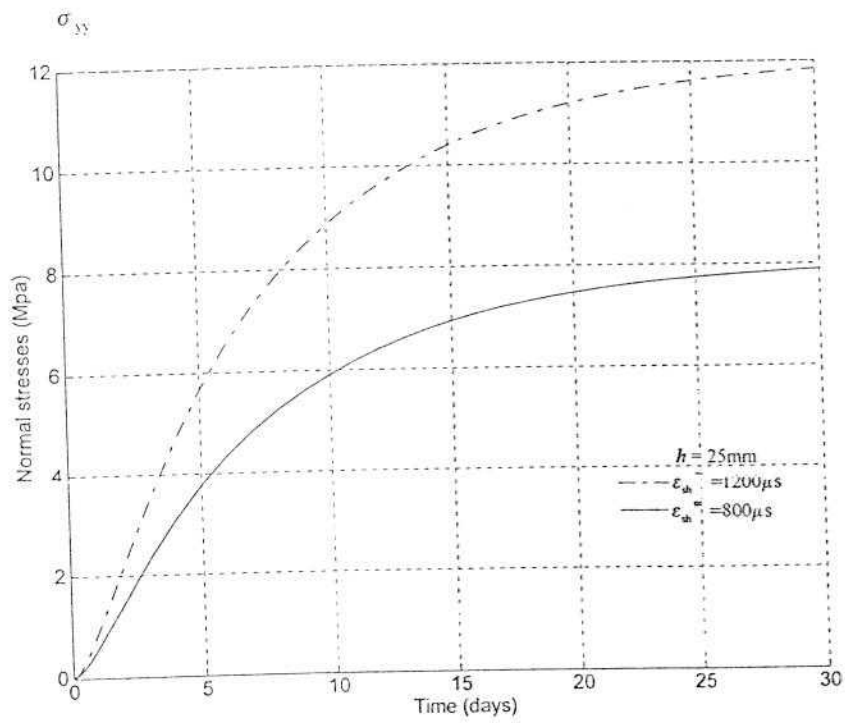


Fig. 6. Variation of  $\sigma_{yy}$  at interface corner ( GP 1 )

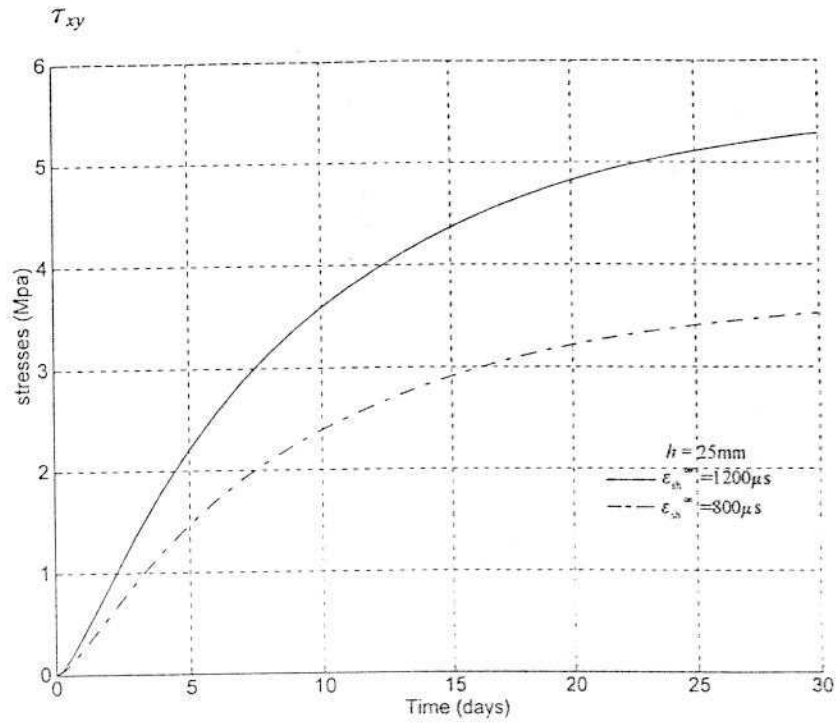


Fig. 7: Variation of  $\tau_{xy}$  at interface corner (GP 1)

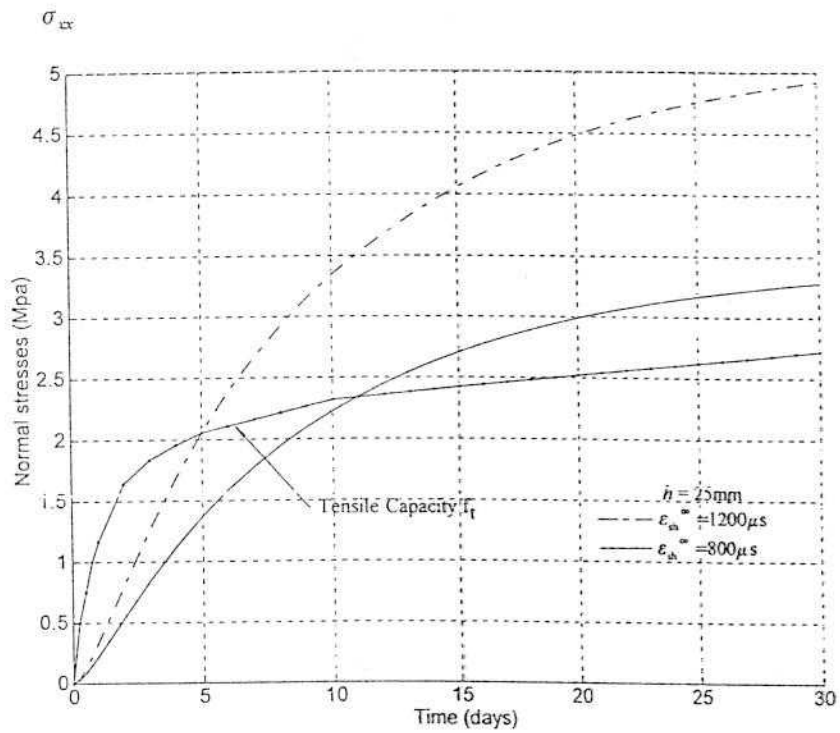


Fig. 8: Time variation of  $\sigma_{xx}$  at top of repair center (GP 900)

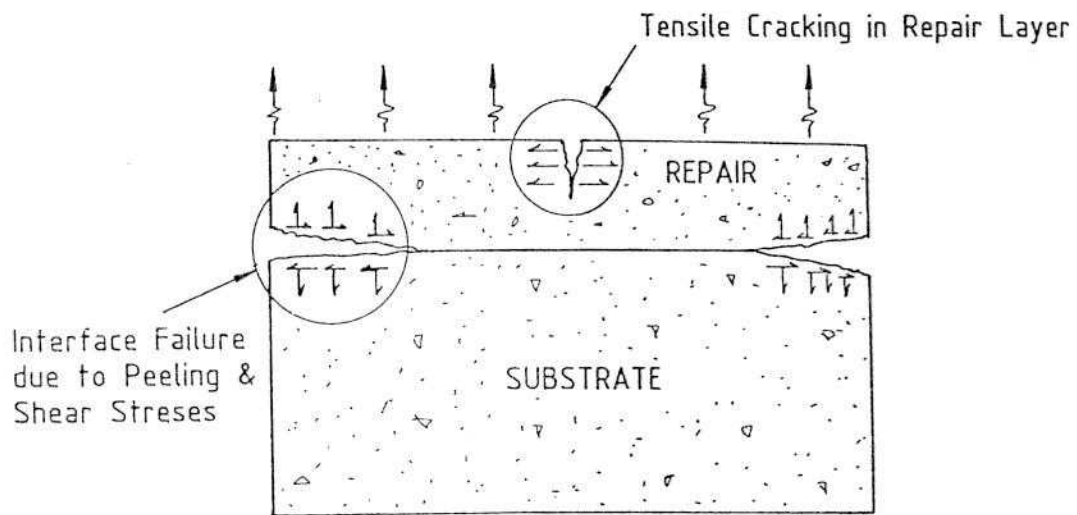


Fig. 9: Identified Modes of Failure